Skin Layer at the Actin-Gel Surface: Quenched Protein Membranes form Flat, Crumpled, and Tubular Morphologies

L. S. Hirst and C. R. Safinya*

Materials & Physics Departments, Biomolecular Science and Engineering Program, University of California, Santa Barbara California 93106, USA

(Received 25 November 2003; published 28 June 2004)

We report the discovery of a hierarchically structured skin layer formed at the surface of an isotropic gel of filamentous actin bundles at high molar ratios of α-actinin, an actin cross-linker, to globular actin. Confocal microscopy has elucidated the full, micron scale 3D structure. The protein skin layer, composed of a directed network of bundles, exhibits flat, crumpled, tubelike and pleated multitubular morphologies, resulting from stresses due to the underlying gel. The skin layer, which readily detaches, constitutes a model anisotropic solid membrane with stress-induced, quenched disorder.

DOI: 10.1103/PhysRevLett.93.018101 PACS numbers: 87.16.Ka, 61.10.Eq, 61.30.Eb, 61.30.St

The actin cytoskeleton provides a structural framework for the mechanical stability of eukaryotic cells and a broad range of cell functions [1]. Actin is found both as monomeric G-actin and as polymerized F-actin filaments. Interactions between F-actin and actin cross-linking proteins (ACPs) may lead to two-dimensional networks and bundles, interacting with the plasma membrane to determine cell shape, or three-dimensional networks imparting gel-like properties to the cytosol. Bundles, comprised of a closely packed parallel arrangement of actin filaments, and networks, containing actin filaments crisscrossed at some large angle, form the most common assembled structures of F-actin [1]. F-actin is a semflexible polyelectrolyte with a linear charge density $\approx -0.4\ e/\text{Å}$ and a persistence length $\approx 10\ \mu$m. The ACP α-actinin is ≈ 3.5 nm wide and ≈ 33 nm long. It forms antiparallel dimers with specific actin-binding regions at each end [2,3]. Thus, α-actinin dimers behave like sticker molecules, bundling F-actin at α-actinin/G-actin molar ratios (γ) of as little as 1/90 at room temperature *in vitro* [4]. We studied F-actin with α-actinin in the limit where F-actin is saturated with α-actinin at molar ratios of $1 < \gamma < 20$. In this regime, approaching negatively charged bundles experience no electrostatic repulsive forces due to the excess sticker concentration and instead the aggregation rate of approaching bundles is determined by an average time between collisions, as in diffusion limited aggregation.

For dilute actin concentrations (~ 0.01 mg/ml) as γ is increased to $\gamma > 1$, we have found that the system undergoes a transition from a sol to an isotropic gel phase of networked actin bundles (i.e., a cluster extending throughout the sample). This bundle gel is distinct from the ubiquitous actin gels found in the cytosol comprised of a network of actin filaments [1]. Most striking is the discovery of dense skin-like structures, formed at the surface of this isotropic gel. Laser scanning confocal microscopy (LSCM) has revealed that on the submillimeter scale, this skin layer may exhibit a range of quenched morphologies including both flat and highly crumpled membranes and tubelike structures. As we describe, the membrane wrinkling is due to stresses resulting from shrinkage of the underlying actin gel to which the skin layer is attached.

We observe that the skin layer comprises a directed network of bundles, oriented over mesoscopic distances. The skin layers, upon detachment from the bulk, present a new class of quenched, protein membranes, irreversibly produced and thus far from equilibrium. This is in contrast with self-assembling equilibrium lipid membranes, found in the form of spherical and cylindrical micelles, flat bilayers, and lipid tubules [5,6]. The protein membranes are experimental realizations of quenched anisotropic solid (i.e., tethered) membranes with disorder due to random stress rather than thermal fluctuations [7].

For microscopy, labeled G-actin was polymerized to a length of $\sim 10\ \mu$m [4]. Complexed α-actinin and actin are shown in Figs. 1(a), 1(a′), and 1(b). A droplet of fluorescently labeled F-actin solution was added to a droplet of α-actinin solution at the required final concentration (0.01 mg/ml F-actin, 100 mM KCl) and ratio. The complexes were then observed using a fluorescence microscope at room temperature. Samples were formed freely suspended in a droplet and sealed with minimal disturbance. At the extremely high ratio $\gamma = 10$, the material exhibits gel-like properties, maintaining shape in solution [Figs. 1(a) and 1(a′)]. Distinct structures can be observed in the complex, and when these samples are deformed the aggregate moves as a single, gelatinous object, resisting shear. In contrast, complexes formed at a relatively low ratio ($\gamma = 1/5$) behave as viscoelastic fluids [Fig. 1(b), sol]. Figures 1(a) and 1(a′) show the same gel sample at two different times in its evolution. Figure 1(a′) after 1 h can clearly be seen to have shrunk in size. Small angle x-ray scattering (SAXS) was performed at the Stanford Synchrotron Radiation Laboratory at 11 keV as described previously [4]. To investigate the internal ordering of actin bundles at high γ,

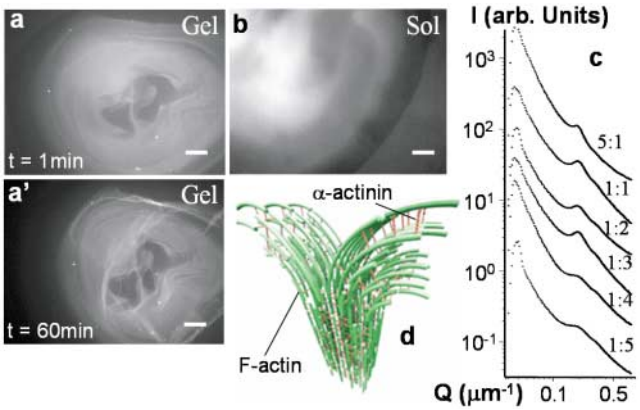

FIG. 1 (color online). Optical fluorescence images (bar = 200 μm) of labeled α-actinin/F-actin mixtures forming gel (a),(a′) and sol (b) samples. (a) $\gamma = 10$ after 1 min, (a′) $\gamma = 10$ after 60 min, and (b) $\gamma = 1/5$. (c) SAXS data for actin bundles, varying the α-actinin/actin ratio (γ) and (d) schematic of the bundle structure.

SAXS experiments were carried out on pelleted gel samples, and scattering data can be seen in Fig. 1(c). The broad peak at $q = 0.2$ nm^{-1} represents a bundle lattice spacing of 31.4 nm, consistent with the length of the α-actinin molecule. On varying γ in the bundled system we observe a hint of a second shoulder peak at 0.28 nm^{-1}. The SAXS data is consistent with the quasi-square lattice arrangement of F-actin within bundles [Fig. 1(d)] found previously for $\gamma < 1$ [4].

Actin filaments are known to form a gel phase at high concentration [8]; however, no gel-like properties on the macroscopic scale of Fig. 1(a) have been observed at the concentrations described here for actin filaments alone (~ 0.01 mg/ml). A higher magnification inspection of this actin/α-actinin gel phase reveals a fascinating architecture of bundle aggregation. Figure 2(a) shows the sample geometry. Figure 2(b) shows LSCM images of α-actinin/actin bundles demonstrating co-localization of F-actin (left) and α-actinin molecules (right). Confocal fluorescence images of a small volume in the gel phase were taken with a resolution of 0.3 μm in the x and y directions and 0.75 μm in the z direction and averaged eight times. Confocal microscopy allows us to fully image the 3D aggregate while suspended in solution, with minimal disturbance to the delicate structures of the sample. Three-dimensional data can then be reconstructed or studied in cross section.

The data in Fig. 2 have been measured for a 158 μm $\times$ 158 μm $\times$ 85 μm volume at $\gamma = 10$. Figure 2(c) shows an x-y projection from above of all actin material in the chosen volume, along with two cross-sectional cuts through the sample in the x-z and y-z planes, as indicated on the figure by black lines. A layer-like bundle distribution in the sample can clearly be seen in the x-z and y-z planes with high concentrations of actin bundles separated by depletion zones. Arrows 1, 2, and 3 designate three volumes in the sample, arrows 1 and 3 indicate volumes containing a sheetlike dense layer, and arrow 2 indicates a depletion zone. From Fig. 2(c) we see there are several highly aligned regions in the sample corresponding to the different layers. The four images to the right in Fig. 2(c) show additional views of the layers indicated by arrows 1 and 2. A projection from above of all material in volume 1 is shown (1-proj), demonstrating more clearly that the actin bundles are highly aligned. Also shown is a projection of the same x-y area but with a

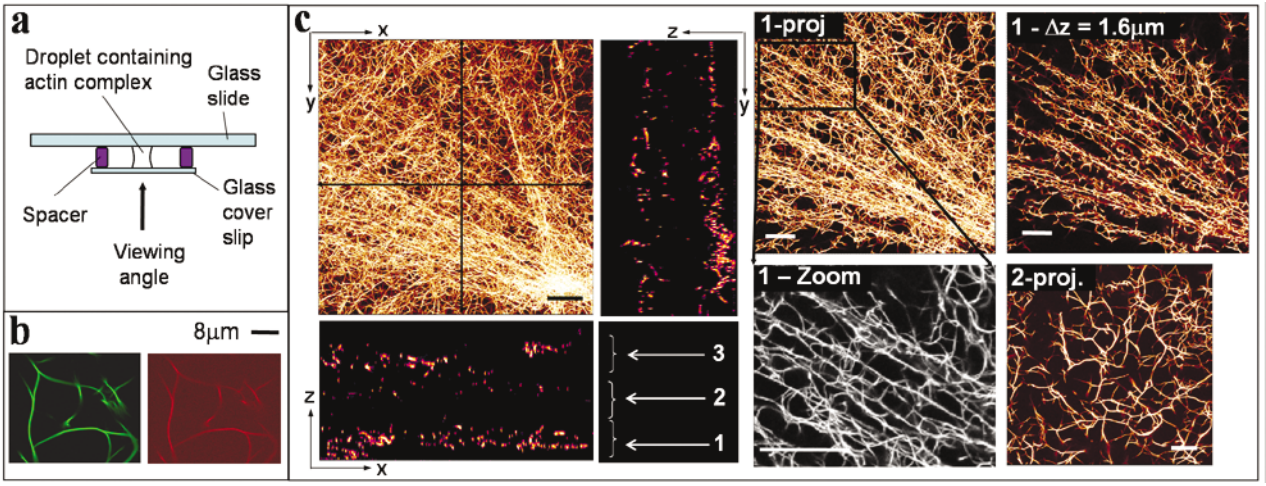

FIG. 2 (color). (a) Schematic of the sample geometry. (b) Co-localization of fluorescent F-actin (left) and α-actinin (right). (c) LSCM images of 3D fluorescence data. Left: the main x-y cross section shows a projection of a $\Delta z = 85$ μm volume inside the α-actinin/actin bundle gel at $\gamma = 10$ with two cross-sectional cuts (x-z and y-z). Three volumes (1, 2, and 3) are marked at different heights in the sample. Right: three different views of volume 1 are shown: a full projection of volume 1 (1-proj), a projection of a thinner section ($1 - \Delta z = 1.6$ μm) of volume 1, and a zoom of the area marked on 1-proj. Also shown is a projection of the volume marked 2 on the main image, showing the isotropic network which connects skin layers 1 and 3 (bars = 20 μm).

smaller depth ($1 - \Delta z = 1.6\ \mu$m). This image shows the actin bundle orientation in more detail and reveals a definite splay in the layer, a feature commonly seen in this system. A higher magnification image of the smaller area marked on 1-proj is also shown (1-zoom). This image demonstrates the ladder-like structure of the dense layers; many strongly oriented bundles, cross-linked into a branching protein network with a mesh size of $\sim 10\ \mu$m, a distance of the order of the persistence length of F-actin. The bottom, right image in Fig. 2(c), (2-proj), shows the projected z range indicated by arrow 2. This depletion volume on closer inspection is a less dense gel comprised of an isotropic network of bundles similar to that observed for lower α-actinin/actin ratios [4]. The isotropic gel regions are observed to be continuous with the more concentrated layer regions, and a combination of both aligned and isotropic ordering is seen throughout the sample with the dense, skin-like layers [arrows 1 and 3, Fig. 2(c)], consisting of a network of aligned bundles, occurring on the surfaces of the isotropic gel [arrow 2, Fig. 2(c)]. Note that data in Fig. 2 show a small volume selection from the gel. The structures are part of much larger layers and represent a typical cross section.

Figure 3 presents a power spectrum analysis of the data in Fig. 2. The structure factor [$S(q)$] was determined using 3D fast Fourier transform (FFT) on LSCM data for a highly aligned region [Fig. 2(c), arrow 1] and a region displaying isotropic ordering [Fig. 2(c), arrow 2]. A slice from the 3D FFT was extracted from the center of the volume in the x-y plane and radial line profiles taken. These profiles were averaged radially about the origin or in the x and y directions and plotted as a function of spatial frequency. By plotting the power spectrum obtained on a log/log plot, a regime with slope 1.72 was observed for the isotropic sample [Fig. 3(a)]. This result is consistent with the slope predicted for cluster-cluster aggregation [9], where the isotropic network of bundles forms as a result of the aggregation of smaller bundle clusters. An analysis was carried out on the aligned volume shown in Fig. 2(c) (arrow 1), with additional curves plotted for intensity profiles in the x and y directions. A similar $S(q)$ linear regime was observed in this sample [Fig. 3(b)], with slightly smaller exponents.

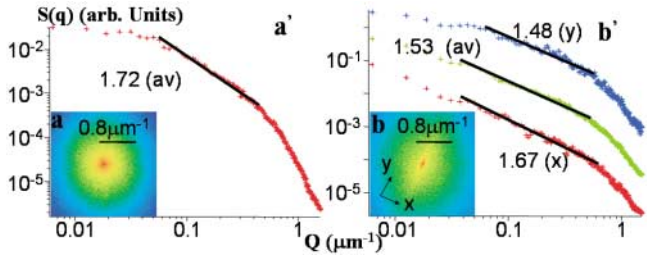

FIG. 3 (color online). Power spectra of data from Figs. 2(a) and 2(b) show x-y slices at $z = 0$ of 3D FFTs of unaligned (2-proj) and aligned (1-proj) regions, respectively. (a′) is a radial plot of (a), azimuthally averaged. (b′) shows radial plots along x, y and azimuthally averaged.

It is apparent that large aligned membrane structures are forming on the surfaces of the isotropic gel and, while actin bundles fluctuate locally between link points, on a macroscopic scale they are locked into a quasirigid configuration with quenched height deviations. In Fig. 4 several examples are presented. LSCM data [Fig. 4(a)] show an anisotropically crumpled membrane structure from a gel sample at $\gamma = 10$. This is an example of a

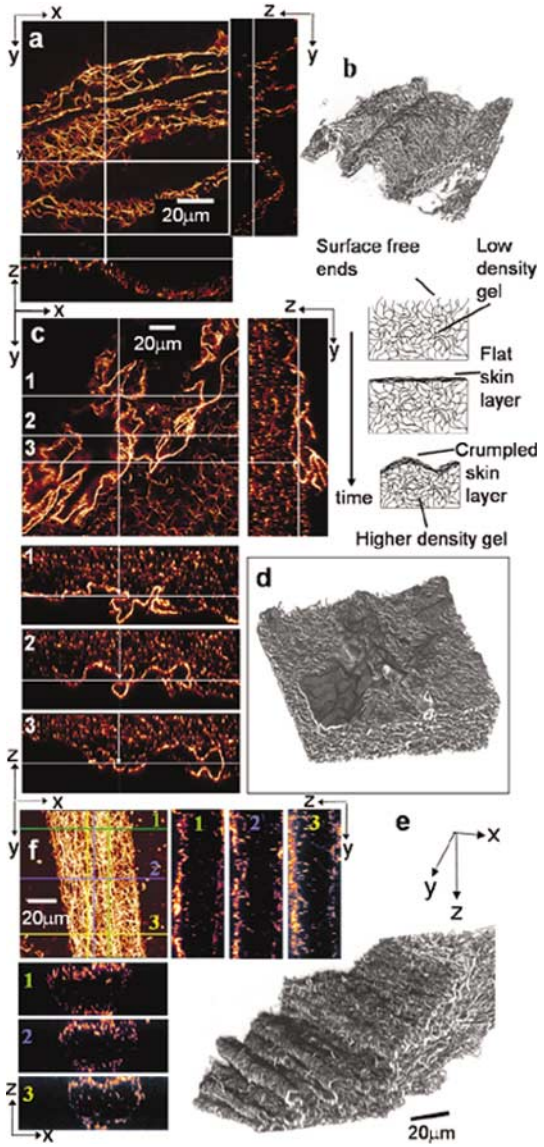

FIG. 4 (color). LSCM data of skin layers on different actin gel samples: (a) a detached layer and (c) at the surface of the actin gel with cross sections as marked, and 3D reconstructions of the data, (b) and (d), respectively, Also shown is a schematic for the mechanism of actin skin formation and wrinkling. (e) 3D reconstruction of a pleated skin layer formed on the actin-gel surface at $\gamma = 10$. (f) LSCM data of a skin layer, separated from the bulk material, forming a large isolated tube at $\gamma = 5$.

surface skin layer which has become detached from the bulk. We also see the membrane in cross section, as marked. In the x-y plane a projection of a small section of the full volume is shown ($\Delta z \sim 3\ \mu$m) with cross sections in the x-z and y-z planes. The z-y plane shows how these height deviations can lead to the formation of tubular structures, a closed-in area having almost formed. Figure 4(b) shows a 3D reconstruction (Voxblast) of the structure. Figure 4(c) shows further LSCM evidence that skin layers may detach from the bulk. A crumpled membrane has formed at $\gamma = 10$ on the surface of an isotropic region. The cross sections (y-z and x-z, 1, 2, and 3) show that the membrane is relatively uniform in thickness (a feature typical of the skin layers) and exhibits a lesser degree of alignment, therefore the crumpling has no preferred direction. The confocal data and 3D rendering [4(d)] show unambiguously that this structure is a membrane composed of a dense network of actin bundles on the surface of the isotropic gel. In some regions the skin has detached from the bulk, allowing a new membrane to form in its place.

The formation of the skin layer may be understood as follows. Upon combining F-actin with α-actinin, bundles begin to form and subsequent cluster-cluster bundle aggregation leads to the isotropic gel. In this high sticker regime ($\gamma > 1$), once a gel is fully formed any loose ends at the surface will eventually fold back due to thermal fluctuations and stick to the surface, creating a dense layer at the gel-water interface. The high bundle concentration at the interface is consistent with orientation observed within the skin layer. The origin of the wrinkled skin layer is revealed by the observation that the gel is shrinking. In this high γ regime the solution is saturated with α-actinin sticker molecules, and if agitated the gel will collapse into a condensed actin pellet as the relatively open, flexible local network sticks to itself and gradually reduces in size. This indicates that the gel phase is locked into a state far from equilibrium, the structure of which is dependent on the initial kinetics of the system. Although the interconnected bundles inside the gel are constrained, thermal fluctuations of the long bundles between link points are readily visible with microscopy. Also, the link points are mobile because α-actinin may slide along F-actin. This combined behavior leads to bundle collisions, thicker bundles, and the observed overall shrinkage. Gel shrinkage is clearly seen in comparing early and late times after preparation (Fig. 1).

Shrinkage of the underlying isotropic gel regions will affect the attached skin layer, which is dense enough to be nearly incompressible and so must buckle under stress to accommodate the shrinkage. An illustration of the process is shown above Fig. 4(d). It is commonly observed that actin skin layers may detach from the bulk to form isolated membranes and tubes. Figure 4(e) shows a 3D rendering of a highly crumpled membrane attached to the bulk gel surface. This is a demonstration of how tubular structures may form by anisotropic crumpling. We can clearly see the ruffled membrane forming several narrow tubes on the surface. Another interesting structure is the large tube in Fig. 4(f), fully detached from the gel. Cross sections in the x-z and y-z planes demonstrate unambiguously the tubelike actin assembly. Tubules from thermally fluctuating anisotropic solid membranes have been predicted theoretically [10] and verified numerically [11], but the work describes phases formed from thermal fluctuations and not heterogeneous stresses as we describe.

The semiflexible protein-membrane skin layers may have applications in templating and tissue engineering either on the gel surface or detached in solution. The skin layer will adapt different shapes, both spontaneously and by controlled manipulation where, in addition to the shapes described here, we have prepared skin layers with spherical morphology. Such structures, including synthetic analogs, could be formed as biological scaffolds, to encapsulate cells or provide a backbone for 3D tissue growth.

We thank R. Bruinsma for insightful discussions. This work was supported by Grants NIH GM-59288; NSF (DMR-0203755, CTS-0103516, and DMR-008034); and DOE (BES) Contract No. W-7405-ENG-34 with the University of California.

*Corresponding author.
Electronic address: safinya@mrl.ucsb.edu

[1] *Molecular Cell Biology*, edited by Lodish *et al.* (Freeman, San Fransisco, 1999); G. C. L. Wong, A. Lin, J. X. Tang, Y. Li, P. A. Janmey, and C. R. Safinya, Phys. Rev. Lett. **91**, 018103 (2003).
[2] M. Imamura *et al.*, J. Biol. Chem. **263**, 7800 (1988).
[3] R. K. Meyer and U. Aebi, J. Cell Biol. **110**, 2013 (1990).
[4] O. Pelletier, E. Pokidysheva, L. S. Hirst, N. Bouxsein, Y. Li, and C. R. Safinya, Phys. Rev. Lett. **91**, 148102 (2003).
[5] J. M. Schnur, Science **262**, 1669 (1993).
[6] B. N. Thomas, C. R. Safinya, R. J. Plano, and N. A. Clark, Science **267**, 1635 (1995).
[7] L. Radzihovshky and D. R. Nelson, Phys. Rev. A **44**, 3525 (1991); D. C. Morse and T. C. Lubensky, Phys. Rev. A **46**, 1751 (1992); D. C. Morse, T. C. Lubensky , and G. S. Grest, Phys. Rev. A **45**, R2151 (1992); P. LeDoussal and L. Radzihovsky Phys. Rev. B **48**, 3548 (1993).
[8] M. Tempel, G. Isenberg, and E. Sackman, Phys. Rev. E **54**, 1802 (1996).
[9] R. Jullien and R. Botet, *Aggregation and Fractal Aggregates* (World Scientific, Singapore, 1987).
[10] L. Radzihovsky and J. Toner, Phys. Rev. Lett. **75**, 4752 (1995); Phys. Rev. B **57**, 1832 (1998).
[11] M. Bowick, M. Falcioni, and G. Thorleifsson, Phys. Rev. Lett. **79**, 885 (1997).